Biosensors and Bioelectronics 30 (2011) 112–117

Contents lists available at SciVerse ScienceDirect

Biosensors and Bioelectronics

journal homepage: www.elsevier.com/locate/bios

One-step "green" preparation of graphene nanosheets and carbon nanospheres mixture by electrolyzing graphite rob and its application for glucose biosensing

Huanshun Yin[a,1], Yunlei Zhou[b,1], Xiaomeng Meng[a], Kun Shang[a], Shiyun Ai[a,*]

[a] College of Chemistry and Material Science, Shandong Agricultural University, Taian, 271018, Shandong, China
[b] College of Life Science, Beijing Normal University, 100875, Beijing, China

ARTICLE INFO

Article history:
Received 28 May 2011
Received in revised form 28 August 2011
Accepted 29 August 2011
Available online 6 September 2011

Keywords:
Direct electrochemistry
Electrolytic graphite rod nanocomposites
Glucose oxidase
Biosensors

ABSTRACT

The graphene nanosheets and carbon nanospheres mixture (GNS–CNS) was prepared by electrolyzing graphite rob in KNO_3 solution under constant current, which was characterized by TEM, AFM, SEM, FT-IR, XRD, XPS, TGA and UV–vis. The nano-mixture can keep stable in water for more than one month. Based on this kind of mixture material, a novel electrochemical biosensing platform for glucose determination was developed. Cyclic voltammetry of glucose oxidase (GOD) immobilized on GNS–CNS/GCE exhibited a pair of well-defined quasi-reversible redox peaks at −0.488 V (E_{pa}) and −0.509 V (E_{pc}) by direct electron transfer between the protein and the electrode. The charge-transfer coefficient (α) was 0.51, the electron transfer rate constant was 2.64 s^{-1} and the surface coverage of HRP was 3.18×10^{-10} mol cm^{-2}. The immobilized GOD could retain its bioactivity and catalyze the reduction of dissolved oxygen. The glucose biosensor has a linear range from 0.4 to 20 mM with detection limit of 0.1 mM. Moreover, the biosensor exhibits acceptable reproducibility and storage stability. The fabricated biosensor was further used to determine glucose in human plasma sample with the recoveries from 96.83% to 105.52%. Therefore, GOD/GNS–CNS/GCE could be promisingly applied to determine blood sugar concentration in the practical clinical analysis.

1. Introduction

Graphene, a new class of two-dimensional nanomaterials, has attracted a great deal of interest in recent years due to its unique electrical, thermal, and mechanical properties, which was widely applied in synthesizing nanocomposites and fabricating various devices, such as capacitors (Du et al., 2010), transistors (Ihn et al., 2010) and solar cell (Hong et al., 2008), especially in electrochemical biosensor. For instance, the direct electrochemistry of glucose oxidase (GOD) was realized on pure graphene nanosheets modified electrode (Wu et al., 2010a). Lu et al. successfully fabricated a H_2O_2 biosensor based on horseradish peroxidase, Nafion and single-layer graphene nanoplatelet modified electrode (Lu et al., 2010). Though the determination purpose of these biosensors have achieved, the weak dispersibility of graphene in water and organic solvents limits their application to a certain degree, because the pure graphene nanosheets tend to aggregate to form graphite through strong π–π stacking and van der Waal's interaction (Shen et al., 2009). Therefore, the graphene dispersion cannot stand for a long time and graphene nanosheets will be precipitated within several hours. As a result, the dispersion needs to be ultrasonicated again before next use.

For avoiding its aggregation, various methods have been developed. Lin's group observed the direct electron transfer of GOD on graphene–chitosan modified glassy carbon electrode (GCE), where chitosan was used as dispersing agent for graphene (Kang et al., 2009). Wang et al. investigated the direct electrochemistry of GOD on graphene–CdS/GCE, in which work, the graphene nanocomposites was dispersed in Nafion solution (Wang et al., 2011). Though the trouble of difficult dispersibility has been solved, the dispersing agents are no-conductivity, which will decrease the conductivity of graphene nanosheets. In order to enhance the dispersity of graphene nanoshets without the aid of chitosan and Nafion, various functionalized graphene nanosheets have been synthesized and applied in biosensor. Niu's group prepared polyvinylpyrrolidone-protected graphene and used it as GOD immobilization matrix to investigate the direct electrochemistry of GOD and glucose biosensing (Shan et al., 2009). Zhang et al. synthesized polymeric ionic liquid functionalized graphene nanosheets, which can well disperse in water and promote the direct electron transfer of GOD (Zhang et al., 2011).

Though the above functionalized graphene nanosheets can well dispersed in water, they are synthesized by chemical reduction of graphene oxide using hydrazine as reductive agent. It is well known that hydrazine is highly toxic, and its use should be extreme care

* Corresponding author. Tel.: +86 538 8247660; fax: +86 538 8242251.
E-mail address: ashy@sdau.edu.cn (S. Ai).
[1] These authors contributed equally to this work.

0956-5663/$ – see front matter © 2011 Elsevier B.V. All rights reserved.
doi:10.1016/j.bios.2011.08.039

and minimized. The chemical process may also leave some residual epoxide groups on the reduced graphene oxide sheets, which leads to some loss in electron mobility (Wang et al., 2009b). Recently, ionic liquid functionalized graphene nanosheets (IL-GNS) are prepared by electrolyzing graphite rod at constant voltage of 15 V using ionic liquid as electrolyte (Liu et al., 2008). The prepared IL-GNS can readily form stable and homogeneous dispersions in polar aprotic solvents such as N,N-dimethylformamide, dimethyl sulfoxide, and N-methylpyrrolidone solution after a brief ultrasonic treatment. However, it cannot longer disperse in water. Encouraged by the preparation of IL-GNS through electrolyzing graphite rod, we prepared the mixture of graphene nanosheets and carbon nanospheres (GNS–CNS) by electrolyzing graphite rob at constant current of 1.0 A using KNO_3 as electrolyte. With the presence of carbon nanospheres, the obtained GNS–CNS can well disperse in water for more than 30 days. In addition, the preparation process is "green" compared with hydrazine reduction, which is hardly any harm to people and environments. For confirming the applicability of GNS–CNS in biosensor, the GOD/GNS–CNS/GCE was fabricated to investigate the direct electrochemistry of GOD. The results indicated that GNS–CNS possess excellent conductivity and adsorptivity. And based on these properties, GNS–CNS can significantly promote the direct electron transfer of GOD. This biosensor also showed good electrocatalytic performance to glucose in O_2-saturated condition with wide linear range, low detection limit and good stability.

2. Experimental

2.1. Material and chemicals

Glucose oxidase (GOD, EC 1.1.3.4, Type X-S, 100 U/mg), flavin adenine dinucleotide (FAD) and D-glucose were purchased from Aladdin (China). The stocked solution of GOD (7 mg/mL) was prepared with 0.1 M phosphate buffer solutions (PBS, pH 7.0) and kept in darkness at 4 °C. A stock solution of D-glucose (0.1 M) was prepared with double distilled deionized water (three-D water) and allowed to mutarotate at room temperature for 24 h before measurements. Working solutions were freshly prepared before use by diluting the stock solution with three-D water. Graphene oxide (GO) was synthesized by chemical oxidation of graphite (Kovtyukhova et al., 1999). Graphene nanosheets were synthesized by chemical reduction of GO with hydrazine according to previous report (Stankovich et al., 2007) and named as RGO. 0.1 M PBS was prepared by mixing the stock solution of 0.1 M NaH_2PO_4 and 0.1 M Na_2HPO_4, and the pH was adjusted by NaOH or HCl. High purity graphite rods were purchased from the Qingdao Tennry carbon Co, Ltd. (China). All chemicals were analytical reagent grade and used without further purification. All solutions were prepared with three-D water from quartz device.

Electrochemical experiments were performed with CHI660C electrochemical workstation (CH Instruments, Inc., USA) with a conventional three-electrode cell. A bare or modified GCE (CHI104, d = 3 mm) was used as working electrode. A saturated calomel electrode (SCE) and a platinum wire were used as reference electrode and auxiliary electrode, respectively. The electrolysis of graphite rob was performed at WLS-5 digital constant-current power (Nanjing, China). The transmission electron microscope (TEM) image was obtained at JEM-2100 TEM (Japan). The scanning electronic microscopy (SEM) was performed on a JEOL-1200EX SEM (Japan). The atomic force microscopy (AFM) measurement was performed on DiMultimode (USA). UV–vis absorbance spectroscopy was performed using a UV-2450 spectrophotometer (Shimadzu Co. Japan). Fourier transform infrared (FT-IR) spectra were recorded with Nicolet 380 spectrometer (Thermo Co., USA). X-ray photoelectron spectroscopy (XPS) was performed on Rigaku D/Max-RB PHI 5000 C ESCA System (USA) using Al Kα 1486.6 eV radiation at 300 W (14 kV). The X-ray powder diffraction (XRD) measurement was taken on a Rigaku D/max-IIB X-ray diffractometer (Japan) with Cu Kα radiation (λ = 1.5418 Å). The thermogravimetric analysis (TGA) was carried out at DTG-60A/60AH thermogravimetric analyzer (Shimadzu, Japan) under N_2 atmosphere at a heating rate of 20 °C/min. All the measurements were carried out at room temperature (25 ± 0.5 °C).

2.2. Preparation of GNS–CNS nano-mixtures

GNS–CNS nano-mixtures were synthesized according to previous report with modification (Lu et al., 2009). In brief, two high-purity graphite rods as electrode were inserted into 50 mL 2.0 M KNO_3 solution prepared with three-D water. After the constant current of 0.2 A was applied to two graphite rods by WLS-5 model constant current meter for 2 h, the constant current was changed to 1.0 A. The anode graphite rod began to corrode and a lot of black precipitate appeared gradually at the bottom of the reactor. Finally, the precipitate was taken out of the reactor after 3 h, washed thoroughly with a lot of water, and then dried at 60 °C in oven for 6 h. The obtained products were named as graphene nanosheets and carbon nanospheres nano-mixtures.

2.3. Preparation of GOD/GNS–CNS/GCE

A GCE was polished to a mirror-like with 0.3 and 0.05 μm alumina slurry on micro-cloth pads, rinsed thoroughly with three-D water between each polishing step, then washed successively with three-D water, anhydrous ethanol and three-D water in an ultrasonic bath and dried in air before use. For preparation of modified electrode, 3 mg/mL GNS–CNS dispersion was first prepared with three-D water, followed by ultrasonication for 1 h. With a microinjector, 5 μL of GNS–CNS dispersion was deposited on the fresh prepared GCE surface. After the solvent was evaporated, the electrode surface was thoroughly rinsed with three-D water and dried in the air. Then 5 μL GOD solution was dropped on the modified electrode surface and dried under room temperature. Then the electrode was rinsed with three-D water to remove the unimmobilized GOD. The obtained electrode was named as GOD/GNS–CNS/GCE. For control, GOD/GCE, GNS–CNS/GCE and FAD/GNS–CNS/GCE were prepared using the similar procedure. The modified GCE was stored at 4 °C in a refrigerator under dry conditions when not in use.

3. Results and discussion

3.1. Characterization of GNS–CNS

The morphologies of GNS–CNS were characterized by TEM (Fig. 1). As can be seen in Fig. 1A–C, GNS–CNS contained graphene nanosheets and carbon nanospheres (average diameter 100 nm). Most carbon nanospheres were adsorbed on the surface and edge of graphene nanosheets. Only little individual graphene nanosheets were observed. The prepared GNS–CNS was also characterized by SEM, AFM, IR, XRD, XPS, TGA and UV–vis (Fig. S1, supplementary material).

3.2. Dispersion of GNS–CNS in water

It is reported that pure graphene nanosheets cannot disperse in water and precipitation of agglomerated nanosheets can be clearly observed through strong π–π stacking and van der Waal's interaction in aqueous solution (Deng et al., 2010). For proving that the dispersion of GNS–CNS in water is superior to graphene nanosheets, the dispersion of GNS–CNS was investigated. As can be seen in Fig. 2A, GNS–CNS can easily be suspended in water after

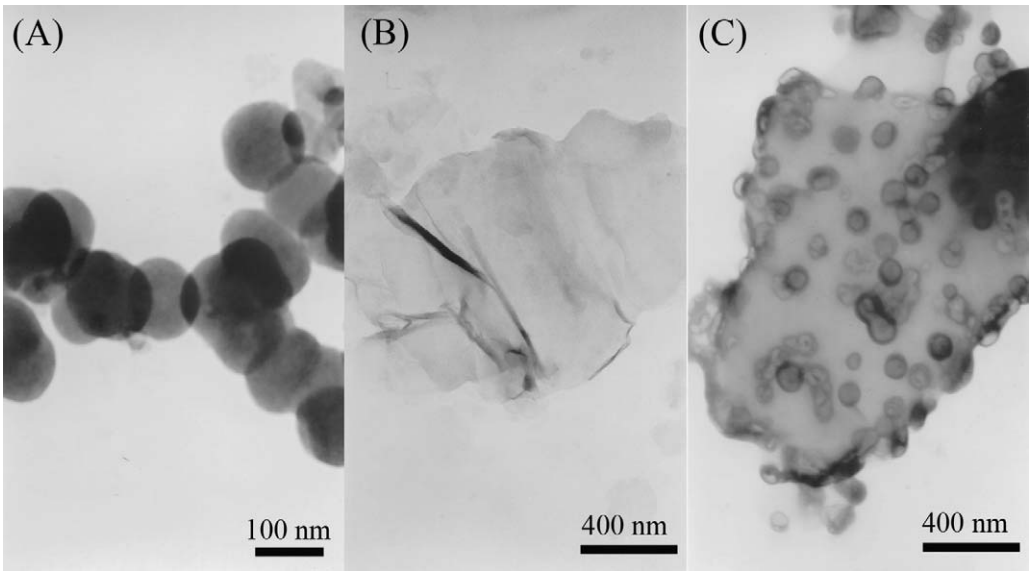

Fig. 1. TEM images of GNS–CNS, in which, (A) carbon nanospheres; (B) graphene nanosheets; and (C) carbon nanospheres was absorbed on grapheme nanosheets.

ultrasonication for 1 h and result a homogeneous black aqueous solution. Such homogeneous suspension is fairly stable and no sign of coagulation of the mixture can be observed even after more than 30 days storage (Fig. 2B). The superior dispersibility of GNS–CNS can be explained as two main reasons. One is that the edge of graphene nanosheets contain hydroxyl and carboxyl, those hydrophilic group can promote the dispersibility of GNS–CNS. In the electrolysis process, the water can be oxidized to form strong oxidants of hydroxyl (•OH) and oxygen radicals (•O), which can attack the graphite edge planes to generate hydroxylation or carboxylation of graphite (Lu et al., 2009). The corrosion process occurs initially at edge sites, grain boundaries, or defect sites and takes place before the expansion of the graphite electrode. In addition, NO_3^- can be reduced at cathode to form NO_2^- and OH^- (Bergmann and Rollin, 2007). After that, the H^+ or OH^- or NO_2^- or NO_3^- in solution can intercalate the interlamination of graphite anode to make it expandation. Finally, some expanded graphite precipitate as graphene sheets or carbon nanospheres with some hydroxyl and carboxyl. The other reason is carbon nanospheres, which was adsorbed on the surface and edge of graphene nanosheets to prevent the aggregation of graphene nanosheets. Though polyvinylpyrrolidone-protected graphene (Shan et al., 2009) and ionic liquid functionalized graphene (Zhang et al., 2011) synthesized by chemical reduction of graphene oxide can also disperse in water and keep stable for months, it must be highlighted that GNS–CNS preparation by electrolysis is very simple and easy compared with the preparation process of the above functionalized graphene. We think that the simple process and the excellent dispersibility in water can increase the application of GNS–CNS in biological and chemical analysis.

Fig. 2. Photographs of GNS–CNS dispersed in water (1 mg/mL) after ultrasonication 1 h (A) and stand for 30 days (B).

3.3. UV–vis spectra of GOD in GNS–CNS dispersion

Though comparing the UV–vis spectra of GOD in GNS–CNS dispersion and FAD–GNS–CNS dispersion, the conclusion can be achieved that the GOD can keep its natural structure in the mixture (Fig. S2, supplementary material).

3.4. Direct electrochemistry of GOD immobilized on the GNS–CNS film

Cyclic voltammetry (CV) was employed to evaluate the performance of the fabricated biosensor. The direct electrochemistry of GOD immobilized on the GNS–CNS/GCE was investigated in 0.1 M nitrogen-saturated PBS (pH 7.0). As shown in Fig. 3a and c, no peak is observed at bare GCE and GNS–CNS/GCE, which indicated that GNS–CNS was electrochemically silent in this potential window. Same to GCE and GNS–CNS/GCE, the redox peaks were not obtained at GOD/GCE (curve b), suggesting that no direct electron transfer of GOD occurred at the bare GCE. However, a pair well-defined redox peaks were observed at GOD/GNS–CNS/GCE (curve d) with the oxidation peak potential (E_{pa}) of −0.488 V and the reduction peak potential of −0.509 V with the peak-to-peak separation (ΔE_p) of 21 mV at 100 mV/s. The ration of the cathodic to anodic current is 1.05, indicating a reversible direct electrochemical oxidation/reduction. The ΔE_p obtained in this work is lower than

Table 1
Performance comparison of the resulting biosensor for the direct electrochemistry of GOD and glucose detection with other biosensors.

Sensor	ΔE_p (mV)	Γ (mol cm^{-2})	Linear range (mM)	LOD (mM)	K_m (mM)	Ref.
Laponite/GOD/GCE	19[d]	2.66×10^{-11}	10–1900	10	–	Shan et al. (2010b)
GOD–graphene–chitosan–CdS/GCE	16[c]	–	2.0–16.0	0.7	1.6	Wang et al. (2011)
Graphene/AuNPs/GOD/chitosan/Au	–	–	2.0–10.0	0.18	–	Shan et al. (2010a)
Nafion/GOD-MC-FDU-15/GCE	27	–	0.1–1	0.09	–	Wang et al. (2009a)
GOD/PPMH/GCE	64	8.50×10^{-11}	0.05–4	0.05	0.64	Oztekin et al. (2011)
CS-GOD-CdS/ACNTs-Pt_{nano} electrode	59[a]	8.0×10^{-10}	0.4–21.2	0.0468	11.86	Yang et al. (2008)
GOD/CILE	56	6.69×10^{-11}	0.1–800	0.03	2.47	Shangguan et al. (2008)
GOD-graphene-chitosan/GCE	80	1.12×10^{-9}	0.08–12	0.02	4.4	Kang et al. (2009)
GOD/Cys/AuNPs/ITO	213	–	0.01–4.8	0.015	12.1	Wang et al. (2008)
GOD-graphene/GCE	27[b]	$1.3 \pm 0.3 \times 10^{-10}$	0.1–10	0.01	–	Wu et al. (2010b)
GOD/SWCNT-Chitosan/GCE	37	1.3×10^{-10}	1–10	0.01	–	Zhou et al. (2008)
Pt/GOx-PVA	–	–	0.1–37	0.01	12.8	Guascito et al. (2011)
GOD/CNx-MWNTs/GCE	7	7.52×10^{-10}	0.02–1.02	0.01	2.2	Deng et al. (2009)
GOD/poly(ViBuIm$^+$Br$^-$)-Graphene/GCE	59[f]	1.45×10^{-11}	0.8–20	0.267	2.4	Zhang et al. (2011)
GOD/BCNTs/GCE	26[e]	1.94×10^{-9}	0.05–0.3	0.01	0.2	Deng et al. (2008)
Nafion-CNTs-CdTe-GOD/GCE	50	8.77×10^{-11}	–	–	0.651	Liu et al. (2007)
Graphite nanosheet-Nafion-GOD/GCE	28	–	0.2–1.4	–	–	Fu et al. (2009)
GOD/GNS–CNS/GCE	21	3.18×10^{-10}	0.4–20	0.1	0.12	This work

[a] 59 mV at 200 mV/s, our work is 25 mV at 200 mV/s.
[b] 27 mV at 40 mV/s, our work is 13 mV at 40 mV/s.
[c] 16 mV at scan rate 50 mV/s, our work is 15 mV at 50 mV/s.
[d] 19 mV at 150 mV/s, our work is 22 mV at 150 mV/s.
[e] 26 mV at 30 mV/s, our work is 11 mV at 30 mV/s.
[f] 59 mV at scan rate 200 mV/s, our work is 25 mV at 50 mV/s.

some previous reports (Table 1), suggesting a faster electrode transfer between the electrode and the redox centers of GOD molecules. It must be highlighted that the ΔE_p obtained in this work is smaller than that at GOD/graphene/GCE and other graphene based electrode (GOD–graphene–chitosan/GCE, GOD/poly(ViBuIm$^+$Br$^-$)-graphene/GCE and GOD–graphene–CdS/GCE), indicating that carbon nanospheres can further improve the electron transfer rate on the base of graphene.

For confirming that whether the direct electron transfer is result from the reduction of FAD linked to the protein or by the reduction of free FAD molecules released from the enzyme, the CV of FAD/GNS–CNS/GCE was also investigated in the same conditions. As can be seen in curve e (Fig. 3), FAD/GNS–CNS/GCE presented a different electrochemical behavior compared with GOD/GNS–CNS/GCE. The oxidation and reduction peaks for FAD/GNS–CNS/GCE were observed at −0.464 and −0.520 V, respectively. The ΔE_p was 56 mV, which was much higher than that at GOD/GNS–CNS/GCE (21 mV), indicating that GOD adsorbed in the GNS–CNS undergoes a more reversible electron transfer process with higher electron transfer rate than that of free FAD adsorbed on GNS–CNS. It is well known that the active redox center of GOD (FAD) is deeply embedded in a protective protein shell, which makes the direct electron communication with electrodes extremely difficult. However, according to the above results, it can be concluded that GNS–CNS can provide a unique microenvironment for the direct electrochemistry of GOD and facilitate direct electron transfer process between the GOD and electrode substrate. In conclusion, the redox waves should be ascribed only to GOD, which is characteristic of reversible electron transfer process of redox active center (FAD) in the GOD (Liu et al., 2005). Moreover, the formal potential ($E_p^{0'}$) of GOD is −0.498 V, which is closed to the value of −0.492 V for free FAD in our work, further confirming that the GOD molecules retain its bioactivity on the modified electrode surface.

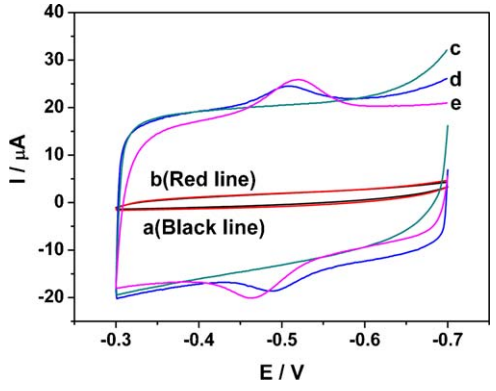

Fig. 3. Cyclic voltammograms of GCE (a), GOD/GCE (b), GNS–CNS/GCE (c), GOD/GNS–CNS/GCE (d) and FAD/GNS–CNS/GCE (e) in N_2-saturated PBS 0.1 M (pH 6.5). Scan rate: 100 mV/s.

It has been reported that the direct electron transfer of GOD is a two-electron and two-proton reaction (Kang et al., 2009). Therefore, the pH effect was investigated. Fig. 4A showed the cyclic voltammograms of GOD/GNS–CNS/GCE in 0.1 M PBS with different pH. The maximum values of the redox peak currents were obtained at pH 7.0, therefore, this pH was chosen as the optimal pH condition. Moreover, a negative shift of the redox peak potentials was observed with increasing pH from 4.0 to 10.0. The formal potential of the redox peak was proportional to the pH with the liner regression equation of $E_p^{0'} = -0.054\ \ \text{pH} - 0.13$ ($R = 0.9972$, Fig. S3, supplementary material). The slope of 54 mV/pH is closed to the theory value of 57.6 mV/pH for a reversible coupled with two-proton and two-electron transfer electrochemical process (Liu et al., 2005), indicating that two-electron and two-proton involve in the redox process of GOD at GNS–CNS/GCE surface.

The effect of scan rate on the direct electrochemistry of GOD was also investigated by cyclic voltammetry. As shown in Fig. 4B, the redox peak current increased with increasing scan rate from 20 to 1000 mV/s. The redox peak current and scan rate showed linear relationship from 20 to 500 mV/s, indicating an adsorption-controlled process in the selected scan rate range (Fig. S4, supplementary material). The corresponding regression equations can be expressed as $I_{pa} = -0.032\nu + 0.49$ ($R = 0.9985$) and $I_{pc} = 0.024\nu + 0.25$ ($R = 0.9968$). The relationship between the peak potential (E_p) and the logarithm value of scan rate ($\log \nu$) was also investigated (Fig. S5, supplementary material). With increasing the scan rate, the oxidation peak potential shifted positively and the reduction peak potential shifted negatively. When $\nu > 200$ mV/s, the E_{pa} and E_{pc} were linearly dependent on the $\log \nu$ with the regression equations of $E_{pa} = -0.05 \log \nu - 0.54$ (V, V/s, $R = 0.9934$)

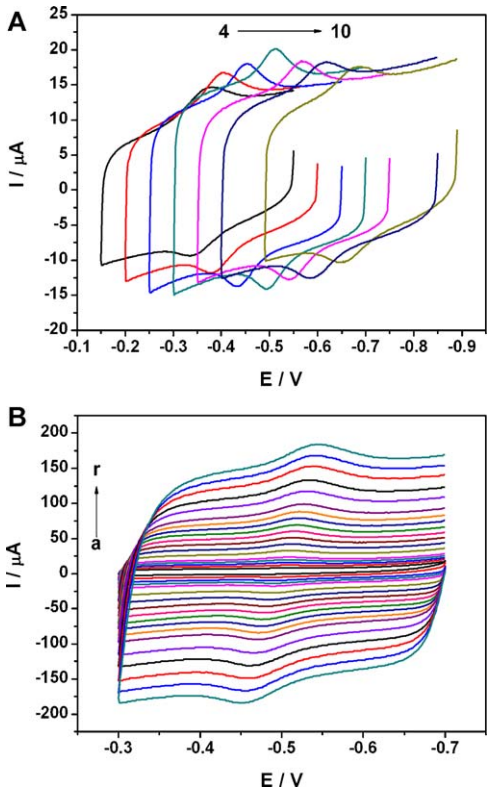

Fig. 4. (A) Cyclic voltammograms of GOD/GNS–CNS/GCE in N_2-saturated 0.1 M PBS at different pH. (B) Cyclic voltammograms of GOD/GNS–CNS/GCE in N_2-saturated 0.1 M PBS (pH 7.0) at different scan rates. a–r: 20, 40, 60, 80, 100, 150, 200, 250, 300, 350, 400, 450, 500, 600, 700,800, 900 and 1000 mV/s.

and $E_{pc} = 0.053 \log \nu - 0.45$ (V, V/s, $R = 0.9844$). According to Laviron theory (Laviron, 1979a) that a plot of E_p versus $\log \nu$ yields two straight lines with slopes of $-2.3RT/\alpha nF$ and $2.3RT/(1-\alpha)nF$ for reduction peak and oxidation peak, respectively, the charge-transfer coefficient, α, can be calculated to be 0.51. In order to calculate the value of apparent heterogeneous electron transfer rate constant (k_s), the following Laviron equation was used (Laviron, 1979a):

$$\log k_s = \alpha \log(1-\alpha) + (1-\alpha)\log\alpha - \log\frac{RT}{nF\nu} - \frac{\alpha(1-\alpha)nF\Delta E_p}{2.3RT} \quad (1)$$

where α is the electron transfer coefficient, n is the number of electron, ΔE_p is the separation of the redox peak, ν is the scan rate. Taking $\alpha = 0.51$, $n = 2$, $\nu = 100$ mV/s and $\Delta E_p = 21$ mV, k_s was calculated to be 2.64 s^{-1}. According to Laviron equation (Laviron, 1979b), $I_p = n^2F^2A\Gamma\nu/4RT$, the surface coverage ($\Gamma$) of GOD on GNS–CNS/GCE is calculated to be 3.18×10^{-10} mol cm^{-2}, which is two orders higher than that of 2.86×10^{-12} mol cm^{-2} at the bare GCE (Liu and Ju, 2003). The Γ obtained in this work is higher than some of previous reports (Table 1). Based on it, the conclusion can be summarized that GNS–CNS can effectively improve the immobilization amount of GOD on the electrode surface.

The effect of the immobilization amount of GNS–CNS and GOD on the direct electrochemistry was also investigated by cyclic voltammetry. The optimal immobilization amount for GNS–CNS and GOD are 3 mg/mL (5 μL) and 7 mg/mL (5 μL), respectively (Figs. S6 and S7, see supplementary material).

3.5. Detection of glucose based on direct electrochemistry of GOD

The above investigation demonstrated that the direct electrochemistry of GOD can be realized on GOD/GNS–CNS/GCE. It has been reported that glucose is the substrate of GOD, which can catalyze glucose to from gluconolactone in the O_2-saturated condition, which can lead to increase the reduced form of GOD and decrease its reduction peak current (Deng et al., 2009; Yang et al., 2011). Based on this, the concentration of glucose can be determined. Therefore, the direct electrochemistry of GOD was carried out in pH 7.0 PBS containing saturated-O_2 and different concentration of glucose. For comparison, the direct electrochemistry of GOD in N_2-saturated PBS was also performed. As can be seen in Fig. 5A, a pair of redox peaks was observed in both N_2 and O_2-saturated PBS. However, the reduction peak current of GOD in O_2-saturated solution was obviously larger than that in N_2-saturated solution, which can be attributed that the electrochemically formed GOD ($FADH_2$) electrocatalyzed the reduction of oxygen, leading to the decreased concentration of GOD ($FADH_2$) (Wang et al., 2011). When glucose was added into the O_2-saturated solution, the reduction peak current of GOD decreased, which can be ascribed to that the addition of glucose triggered the GOD-catalyzed oxidation reaction for glucose in the presence of O_2 and decrease the oxidation form of GOD (FAD). Therefore, the oxidation peak current of GOD decreased. For further proving that catalytic activity of the prepared electrode, the CV of GOD/GNS–CNS/GCE in 0.1 M pH 7.0 PBS containing different concentration of glucose with N_2 saturation was investigated. The results indicated that the redox peak current of GOD almost did not change before and after addition of glucose with the same concentrations to Fig. 5A (Fig. S8, see supplementary material). This result further confirmed that the catalytic activity of GOD only existed in the presence of O_2, which should act as enzymatic reaction medium. With changing the glucose concentration from 0.4 to 20 mM in O_2-satureated pH 7.0 PBS, a linear relationship between the change of the reduction peak current of GOD and the glucose concentration can be obtained with the regression equation of $\Delta I_{pc} = 0.017c + 0.12$ ($R = 0.9909$, Fig. 5B). The detection limit is 0.1 mM (S/N = 3). The determination performance of GOD/GNS–CNS/GCE was compared with other GOD biosensor and the results were shown in Table 1. It can be seen that GOD/GNS–CNS/GCE showed a rational linear range and relative low detection limit. The apparent Michalis–Menten constant (K_m) was calculated to be 0.12 mM according to the Lineweaver–Burk equation (Kamin and Wilson, 1980), which is smaller than some previous reports (Table 1). The smaller K_m value indicates that the immobilized GOD possesses higher enzymatic activity and the GOD/GNS–CNS/GCE exhibits a higher affinity for glucose.

The possible interference species on the detection of glucose, such as uric acid and ascorbic acid, were studied. The results showed that 0.5 mM uric acid and 0.1 mM ascorbic acid did not cause any interference to 1.0 mM glucose determination. The detection reproducibility of the glucose biosensor was investigated by successively detecting 1.0 mM glucose for 5 times, the relative standard deviation (RSD) was 4.88%, demonstrating a good reproducibility. The fabrication reproducibility for six GOD/GNS–CNS/GCE was investigated by comparing the oxidation peak current of 1 mM glucose. The RSD is 4.74%, indicating an acceptable reproducibility. The fabrication reproducibility of GOD/GNS–CNS/GCE was also investigated by comparing the redox peak current of GOD in the absence of O_2 and glucose. The RSD is 4.34% and 5.01% for oxidation peak current and reduction peak current for six electrodes fabricated independently, respectively. The stability of GOD/GNS–CNS/GCE was evaluated by examining the cyclic voltammetric peak currents of GOD after continuously scanning. It was found that the peak current almost remained 98.87% of the initial response after 100 cycles, indicating the excellent

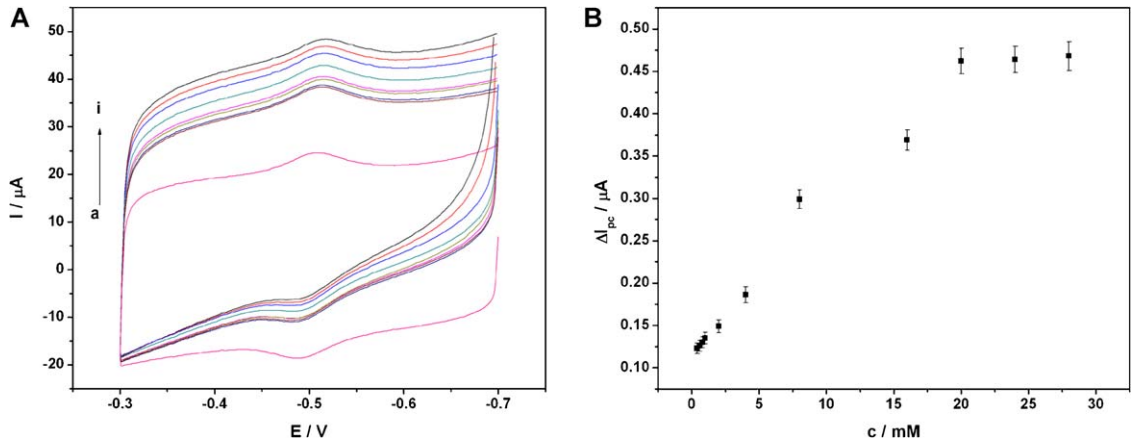

Fig. 5. (A) Cyclic voltammograms of GOD/GNS–CNS/GCE in nitrogen-saturated (a) and oxygen-saturated (b–i) 0.1 M pH 7.0 PBS in the absence (a, i) and presence of 2.0 (h), 4.0 (g), 8 (f), 16 (e), 24 (d), 28 (c) and 32 mM (b) glucose at 100 mV/s. (B) Calibration curve for glucose determination.

stability in PBS. Moreover, the stability was also investigated by storing the modified electrode in pH 7.0 PBS at 4 °C. The cyclic voltammetry were performed every 7 days. After being stored for 14 days, the reduction peak current only decreased 9.26% for 1.0 mM glucose, suggesting the acceptable stability.

3.6. Determination of glucose in human plasma sample

It is well known that a diagnostic criterion for diabetes is fasting blood glucose higher than 7.0 mM and/or postprandial blood glucose higher than 11.0 mM. Therefore, the linear range (0.4–20 mM) for glucose determination in our work is suitable for blood glucose concentration determination. For achieving it, 1 mL human plasma sample was added into 9 mL PBS, then, the cyclic voltammetry was performed. The concentration of glucose was determined to be 6.12 mM with RSD of 4.18%. The recoveries are between 96.83% and 105.52% for three times determination.

4. Conclusion

In this work, the graphite rod was electrolyzed in 2 M KNO_3 aqueous solution. The obtained electrolysis products (GNS–CNS) were used as matrix for GOD immobilization. The investigations reveal that GNS–CNS can provide a unique microenvironment for GOD to maintain its bioactivity and facilitate the electron transfer between GOD and electrode. Based on this, the direct electrochemistry of GOD was realized. The glucose determination was achieved by the decrease of the reduction peak current of GOD in the O_2-saturated PBS with addition of glucose. The biosensor showed good determination performance when compared with previous reports.

Acknowledgements

The authors thank the National Natural Science Foundation of China (no. 21075078) and the Natural Science Foundation of Shandong province of China (no. ZR2010BM005) for the financial supports.

Appendix A. Supplementary data

Supplementary data associated with this article can be found, in the online version, at doi:10.1016/j.bios.2011.08.039.

References

Bergmann, M., Rollin, J., 2007. Catal. Today 124 (3–4), 198–203.
Deng, C., Chen, J., Chen, X., Xiao, C., Nie, L., Yao, S., 2008. Biosens. Bioelectron. 23 (8), 1272–1277.
Deng, S., Jian, G., Lei, J., Hu, Z., Ju, H., 2009. Biosens. Bioelectron. 25 (2), 373–377.
Deng, X., Lili, L., Li, H., Luo, F., 2010. J. Hazard. Mater. 183 (1–3), 923–930.
Du, X., Guo, P., Song, H., Chen, X., 2010. Electrochim. Acta 55 (16), 4812–4819.
Fu, C., Yang, W., Chen, X., Evans, D.G., 2009. Electrochem. Commun. 11 (5), 997–1000.
Guascito, M.R., Chirizzi, D., Malitesta, C., Mazzotta, E., 2011. Analyst 136 (1), 164–173.
Hong, W., Xu, Y., Lu, G., Li, C., Shi, G., 2008. Electrochem. Commun. 10 (10), 1555–1558.
Ihn, T., Güttinger, J., Molitor, F., Schnez, S., Schurtenberger, E., Jacobsen, A., Hellmüller, S., Frey, T., Dröscher, S., Stampfer, C., Ensslin, K., 2010. Mater. Today 13 (3), 44–50.
Kamin, R.A., Wilson, G.S., 1980. Anal. Chem. 52 (8), 1198–1205.
Kang, X., Wang, J., Wu, H., Aksay, I.A., Liu, J., Lin, Y., 2009. Biosens. Bioelectron. 25 (4), 901–905.
Kovtyukhova, N.I., Ollivier, P.J., Martin, B.R., Mallouk, T.E., Chizhik, S.A., Buzaneva, E.V., Gorchinskiy, A.D., 1999. Chem. Mater. 11 (3), 771–778.
Laviron, E., 1979a. J. Electroanal. Chem. 101 (1), 19–28.
Laviron, E., 1979b. J. Electroanal. Chem. 100, 263–270.
Liu, N., Luo, F., Wu, H., Liu, Y., Zhang, C., Chen, J., 2008. Adv. Funct. Mater. 18 (10), 1518–1525.
Liu, Q., Lu, X., Li, J., Yao, X., 2007. Biosens. Bioelectron. 22 (12), 3203–3209.
Liu, S., Ju, H., 2003. Biosens. Bioelectron. 19 (3), 177–183.
Liu, Y., Wang, M., Zhao, F., Xu, Z., Dong, S., 2005. Biosens. Bioelectron. 21 (6), 984–988.
Lu, J., Yang, J., Wang, J., Lim, A., Wang, S., Loh, K.P., 2009. ACS Nano 3 (8), 2367–2375.
Lu, Q., Dong, X., Li, L.-J., Hu, X., 2010. Talanta 82 (4), 1344–1348.
Oztekin, Y., Ramanaviciene, A., Yazicigil, Z., Solak, A.O., Ramanavicius, A., 2011. Biosens. Bioelectron. 26 (5), 2541–2546.
Shan, C., Yang, H., Han, D., Zhang, Q., Ivaska, A., Niu, L., 2010a. Biosens. Bioelectron. 25 (5), 1070–1074.
Shan, C., Yang, H., Song, J., Han, D., Ivaska, A., Niu, L., 2009. Anal. Chem. 81 (6), 2378–2382.
Shan, D., Zhang, J., Xue, H.-G., Ding, S.-N., Cosnier, S., 2010b. Biosens. Bioelectron. 25 (6), 1427–1433.
Shangguan, X., Zhang, H., Zheng, J., 2008. Electrochem. Commun. 10 (8), 1140–1143.
Shen, J., Hu, Y., Li, C., Qin, C., Ye, M., 2009. Small 5 (1), 82–85.
Stankovich, S., Dikin, D.A., Piner, R.D., Kohlhaas, K.A., Kleinhammes, A., Jia, Y., Wu, Y., Nguyen, S.T., Ruoff, R.S., 2007. Carbon 45 (7), 1558–1565.
Wang, J., Wang, L., Di, J., Tu, Y., 2008. Sens. Actuators B 135 (1), 283–288.
Wang, K., Liu, Q., Guan, Q.-M., Wu, J., Li, H.-N., Yan, J.-J., 2011. Biosens. Bioelectron. 26 (5), 2252–2257.
Wang, K., Yang, H., Zhu, L., Ma, Z., Xing, S., Lv, Q., Liao, J., Liu, C., Xing, W., 2009a. Electrochim. Acta 54 (20), 4626–4630.
Wang, Z., Zhou, X., Zhang, J., Boey, F., Zhang, H., 2009b. J. Phys. Chem. C 113 (32), 14071–14075.
Wu, P., Shao, Q., Hu, Y., Jin, J., Yin, Y., Zhang, H., Cai, C., 2010a. Electrochim. Acta 55 (28), 8606–8614.
Wu, P., Shao, Q., Hu, Y., Jin, J., Yin, Y., Zhang, H., Cai, C., 2010b. Electrochim. Acta 55, 8606–8614.
Yang, J., Zhang, R., Xu, Y., He, P., Fang, Y., 2008. Electrochem. Commun. 10 (12), 1889–1892.
Yang, Z., Ren, Y., Zhang, Y., Li, J., Li, H., Hu, X.H.X., Xu, Q., 2011. Biosens. Bioelectron. 26 (11), 4337–4341.
Zhang, Q., Wu, S., Zhang, L., Lu, J., Verproot, F., Liu, Y., Xing, Z., Li, J., Song, X.M., 2011. Biosens. Bioelectron. 26 (5), 2632–2637.
Zhou, Y., Yang, H., Chen, H.Y., 2008. Talanta 76 (2), 419–423.